Ed.) pp 457-466, Academic Press, New York.
Illuminati, G., & Mandolini, L. (1981) *Acc. Chem. Res. 14*, 95-102.
Johnson, W. C., Jr. (1990) *Proteins: Struct., Funct., Genet. 7*, 205-214.
Kawahara, K., & Tanford, C. (1966) *J. Biol. Chem. 241*, 3228-3232.
Kim, P. S., & Baldwin, R. L. (1980) *Biochemistry 19*, 6124-6129.
Kim, P. S., & Baldwin, R. L. (1984) *Nature 307*, 329-334.
Kim, P. S., & Baldwin, R. L. (1990) *Annu. Rev. Biochem. 59*, 631-660.
King, J. (1989) *Chem. Eng. News 67*, 32-54.
Kirby, A. J. (1980) *Adv. Phys. Org. Chem. 17*, 183-278.
Levitt, M. (1978) *Biochemistry 17*, 4277-4285.
Lin, T.-Y., & Kim, P. S. (1989) *Biochemistry 28*, 5282-5287.
Marqusee, S., Robbins, V. H., & Baldwin, R. L. (1989) *Proc. Natl. Acad. Sci. U.S.A. 86*, 5286-5290.
Oas, T. G., & Kim, P. S. (1988) *Nature 336*, 42-48.
Pace, C. N., & Creighton, T. E. (1986) *J. Mol. Biol. 188*, 477-486.
Pease, J. H. B., & Wemmer, D. E. (1988) *Biochemistry 27*, 8491-8498.
Riddles, P. W., Blakeley, R. L., & Zerner, B. (1979) *Anal. Biochem. 94*, 75-81.
Roder, H., Elove, G. A., & Englander, S. W. (1988) *Nature 335*, 700-704.
Shoemaker, K. R., Kim, P. S., York, E. J., Stewart, J. M., & Baldwin, R. L. (1987) *Nature 326*, 563-567.
Snyder, G. H. (1987) *Biochemistry 26*, 688-694.
States, D. J., Creighton, T. E., Dobson, C. M., & Karplus, M. (1987) *J. Mol. Biol. 195*, 731-739.
Szajewski, R. P., & Whitesides, G. M. (1980) *J. Am. Chem. Soc. 102*, 2011-2026.
Udgaonkar, J. B., & Baldwin, R. L. (1988) *Nature 335*, 694-699.
Wemmer, D., & Kallenbach, N. R. (1983) *Biochemistry 22*, 1901-1906.
Zhang, R., & Snyder, G. H. (1988) *Biochemistry 27*, 3785-3794.
Zhang, R., & Snyder, G. H. (1989) *J. Biol. Chem. 264*, 18472-18479.

pH-Induced Folding/Unfolding of Staphylococcal Nuclease: Determination of Kinetic Parameters by the Sequential-Jump Method†

Hueih M. Chen, Vladislav S. Markin, and Tian Yow Tsong*
Department of Biochemistry, University of Minnesota College of Biological Sciences, St. Paul, Minnesota 55108
Received June 18, 1991; Revised Manuscript Received October 25, 1991

ABSTRACT: On the basis of previous stopped-flow pH-jump experiments, we have proposed that the acid- and alkaline-induced folding/unfolding transition of staphylococcal nuclease, in the time range 2 ms to 300 s, follows the pathway $N_0 \rightleftharpoons D_1 \rightleftharpoons D_2 \rightleftharpoons D_3$, in which D_1, D_2, and D_3 are three substates of the unfolded state and N_0 is the native state. The stopped-flow "double-jump" technique has been employed to test this mechanism and to determine the rate constants which would not be accessible by the direct pH jump because of the lack of fluorescence signal, i.e., the rates for the conversion of D_1 to D_2 and of D_2 to D_3. In the forward jump, a protein solution kept at pH 7.0 was mixed with an acidic or alkaline solution to the final pH of 3.0 or 12.2, respectively. The mixed solution was kept for varying periods of time, called the delay time, t_D. A second mixing (the back jump) was launched to bring the protein solution back to pH 7.0. The time course of the Trp-140 fluorescence signals recovered in the back jump was analyzed as a function of t_D. Kinetics of the unfolding were found to be triphasic by the double-jump method, contrary to the monophasic kinetics observed by the direct pH jump. Complex kinetics of unfolding are expected with the proposed kinetic scheme. Analysis of data obtained by both the direct-jump and the double-jump experiments yielded complete sets of rate constants and activation energies for the unfolding to pH 3.0 and to pH 12.2 and for the folding from acid and alkali to pH 7.0. Fractions of protein in N_0, D_1, D_2, and D_3 states were determined to be 1.0, 0, 0, and 0, respectively, at pH 7.0; 0, 0.61, 0.28, and 0.11, respectively, at pH 3.0; and 0, 0.43, 0.30, and 0.27, respectively, at pH 12.2. ΔG of the transition between any two neighbors of the three D's was less than 0.55 kcal mol^{-1}. Thus, any obligatory pathway in an early stage of the chain folding must be determined by the kinetic barriers rather than by the stability of the intermediate states.

Staphylococcal nuclease (SNase) is a classical protein for the study of protein folding because of several convenient features. First, it consists of one peptide chain and is a single-domain protein of relatively small molecular weight, 16 800 (149 residues). Thus, its stability and pathway for folding should be more amenable to biophysical study than proteins of more complex structure. Second, there are no disulfide bridges in the structure. The unfolded peptide should behave closely like an ideal random polymer chain (Tanford, 1968). Any peptide/solvent interaction would be easier to analyze. Third, many single, double, or multiple amino acid substituted mutants are available. By comparative study of these mutants, the contribution of individual amino acids to the stability of the protein or the pathway of folding may be assessed (Shortle, 1989).

Kinetics of the folding/unfolding of SNase have been investigated in several laboratories. Schechter et al. (1970) and Epstein et al. (1971) have studied folding of the protein from

† This work was supported by NIH Grant GM 37304.

0006-2960/92/0431-1483$03.00/0

acid and found a nucleation reaction in the 50-ms and a folding reaction in the 550-ms time ranges. Davis et al. (1979) have compared the folding kinetics of SNase with another species, SNase B, and reported that the reaction of SNase is more complex than those reported previously; i.e., there are three, instead of two, kinetic phases in the folding. The third phase has a time constant of 35 s. Nakano and Fink (1990) examined effects of low temperatures and cosolvents, such as methyl alcohol and GdnSCN, on rates of these three kinetic phases. These studies monitored fluorescence increase of Trp-140 upon folding. Sugawara et al. (1991) have studied folding from the urea-unfolded state by following the recovery of the ellipticity (CD) of the peptide backbone. Their main finding is the formation of 30% helical structure within the 15-ms mixing time of the CD stopped-flow instrument. They have also studied effects of Ca^{2+} and thymidine 3′,5′-diphosphate on the folding process.

Our previous study focused on characterizing the nature of the unfolded state (Chen et al., 1991). From the comparison of the equilibrium unfolding study by differential scanning calorimetry (DSC), circular dichroism (CD), and fluorescence spectroscopy and from the kinetics of unfolding to acid or alkaline conditions and folding from these conditions to pH 7.0, we concluded that whereas the native state of SNase is an unique state, by the criteria of DSC and CD and fluorescence spectroscopies, the unfolded state is composed of three substates, D_1, D_2, and D_3. These substates of the denatured state have similar Trp-140 fluorescence, and conversion among them cannot be detected by Trp-140 fluorescence. Since no heat of transition was detectable by heating the protein from 10 to 80 °C, at pH 3.0 or pH 12.2, these three substates of the denatured protein are considered to have a similar enthalpy function. In other words, there is no ΔH of transition among any of the three substates. However, these substates are distinguished by the kinetic barriers among them, and their state differences are purely entropic (Chen et al., 1991). A simple sequential model (Scheme I) has been proposed to interpret these observations. The rate constants for all three steps in folding, from acid and alkaline conditions to pH 7.0, and for the N_0 to D_1 step in unfolding, from pH 7.0 to pH 3.1 and 11.45, have been determined (Chen et al., 1991). However, because of the lack of fluorescence signal associated with $D_1 \rightarrow D_2 \rightarrow D_3$ transitions, rate constants for these two unfolding steps could not be determined. They can only be measured by an indirect method, i.e., the double-jump method (Brandts et al., 1975; Hagerman & Baldwin, 1976). Also, experimental proof of Scheme I cannot be done unambiguously by the direct-jump method alone. A more stringent test can only be effected by the double-jump method (Hagerman & Baldwin, 1976).

Scheme I

$$N_0 \rightleftharpoons D_1 \rightleftharpoons D_2 \rightleftharpoons D_3$$

Materials and Methods

Material. Escherichia coli strain AR120 carrying the recombinant plasmid pL9 containing the nuclease gene was the gift of Dr. David Shortle of the Johns Hopkins University School of Medicine. The *E. coli* was grown in a 120-L batch size fermentor in the College of Biological Sciences facility. The protein was purified according to the procedure of Shortle and Meeker (1989). The purity of protein was checked by SDS–polyacrylamide gel electrophoresis and was judged to be greater than 98%. The concentration of the protein was determined by a Perkin-Elmer λ 5 spectrophotometer using the optical density at 280 nm (0.93 at 1 mg/mL) (Fuchs et al., 1967).

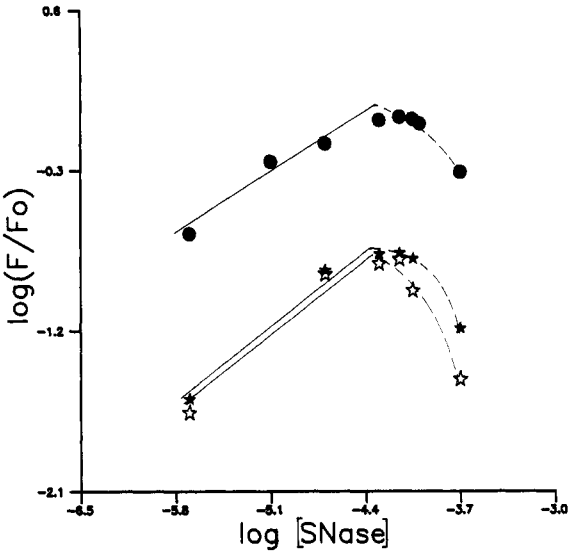

FIGURE 1: Tryptophan fluorescence, in arbitrary units, as a function of protein concentration. Data in closed circles, open stars, and filled stars are for SNase at pH 7.0, 11.6, and 2.8, respectively. Fluorescence was measured with an Aminco-Bowman spectrofluorometer, with the excitation beam set at 285 nm and emission monitored at 335 nm. The temperature was 25 °C. The solvent contained 0.12 M NaCl and 0.05 M phosphate buffer, adjusted to the desired pH by 6 M HCl or 6 M NaOH. At 70 μM (1.18 mg/mL), the fluorescence intensity was no longer proportional to [SNase], indicating protein aggregation and other unrelated fluorescence quenching. All kinetic experiments were done with an initial protein concentration of less than 60 μM.

Kinetic Measurements. A Hi-Tech Model PQ/SF-53 stopped-flow instrument with a multiple mixing attachment was used. The instrument has a nominal mixing time of 0.8 ms for an observation chamber with a path length of 2 mm. The baseline of the instrument was stable, and the drift was small for the time range from 2 ms to 500 s. Tryptophan fluorescence (Trp-140) was used to monitor the kinetics. Excitation beam was set at 285 nm, and the emission integrated above 300 nm was followed. Signals were digitized (12-bit resolution) and analyzed with an IBM-compatible PC. In the sequential-jump experiments, after the first mixing from pH 7.0 to a final pH of 3.0 or 12.2, the flow was stopped for a period of time called the delay time, t_D, and then a second pneumatic drive was activated. This second mixing brought the final mixture of the protein solution back to the initial pH 7.0. The range of t_D accessible with the kinetic instrument is 10 ms to several hundred seconds. All mixings were with an equal volume so that the initial concentration of protein was diluted 2-fold in the first mixing and further diluted 2-fold in the second mixing. The final concentration of protein was 0.15 mg/mL. Kinetics were followed by changes in the fluorescence of the single Trp-140, as was described previously (Chen et al., 1991). The intensity of the fluorescence is a linear function of the protein concentration up to 1.18 mg/mL (70 μM). At higher concentrations, there was either an aggregation of protein or other quenching, and the fluorescence intensity diminished with increasing protein concentration (Figure 1). Thus, in the concentration range studied, protein aggregation was insignificant. Also, the acid- and alkaline-induced folding/unfolding transitions were completely reversible (Chen et al., 1991). All kinetic measurements were done in the presence of 0.12 M NaCl and 0.05 M potassium phosphate at 25 °C. A buffer containing a suitable amount of HCl or NaOH was mixed to bring the protein solution to a desired pH.

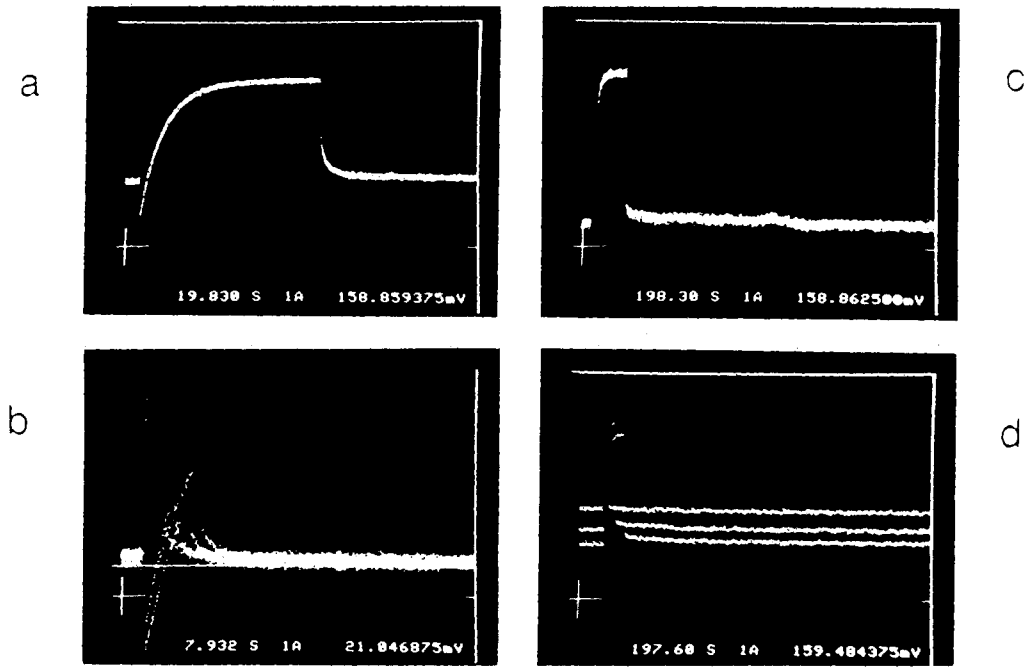

FIGURE 2: Kinetic records of the acid-induced unfolding/refolding transitions by the sequential pH jumps. (a) The initial solution (protein concentration 0.6 mg/mL at pH 7.0) was mixed with a buffer of pH 1.9 to bring the pH to 3.0. After 10 s (t_D), the solution was mixed a second time with a buffer at pH 10.5 that brought the pH of the final mixture back to 7.0. The fluorescence change, excited at 285 nm and monitored above 300 nm, in the unfolding jump is given in the upward curve (a decrease in fluorescence intensity), and that in the refolding jump is in the downward curve (an increase in fluorescence). The first 10 s after the second mixing is recorded. The final protein concentration was 0.15 mg/mL. (b) Kinetic records similar to that in (a) but with t_D of 1.0, 0.8, 0.5, and 0.3 s, for upper to lower traces, respectively, are shown. The recording time was 8 s. (c) Kinetic record of a refolding jump after t_D of 20 s is shown. The total recording time was 200 s. (d) More kinetic records are shown of the slow kinetic phase in the refolding jump, with t_D of 1.2, 5, and 10 s, respectively, from the upper to the lower trace. The total recording time was 200 s. All measurements were done at 25 °C.

Since kinetics are complex, except for the unfolding to strongly denaturing conditions, i.e., to pH < 3 or pH > 11.5, which were monophasic (Chen et al., 1991), a nonlinear least-squares program supplied by the manufacturer of the stopped-flow instrument was used to deconvolute a kinetic record into a minimum number of exponential decays. The method is based on the algorithm of Marquardt (1963). Typically, a kinetic record from 2 ms to 5 s was fit into two exponential decays, and that from 5 s to 300 s was fit into one exponential decay. In the double-jump experiment, the fluorescence signals recovered in the second jump gave triphasic kinetics in the time range 2 ms to 300 s. The amplitude of the three kinetic phases in the refolding jump depended on t_D and was analyzed according to the method described in the Results section and the Appendix. The details of deconvolution of a kinetic record are given elsewhere (Chen et al., 1991).

Results and Analysis

Double-Jump Experiments. Typical fluorescence signals associated with the unfolding of SNase are shown in the upward curves of oscillographs a in Figure 2 for unfolding from pH 7.0 to pH 3.0 and in Figure 3 for unfolding from pH 7.0 to pH 12.2. The downward curves in the same oscillographs recorded kinetics of the second jump, or the refolding jump, to pH 7.0 after a 10-s delay time. In both cases, the fluorescence signals for the equilibrium unfolding were nearly completely recovered after the correction of the 2-fold dilution due to the stopped-flow mixing of the sample solution. This is expected because the N_0 to D_1 transition in the unfolding to pH 3.0 or pH 12.2 was relatively fast for the protein (Davis et al., 1979; Nakano & Fink, 1990; Sugawara et al., 1991; Chen et al., 1991). Thus, during the 10-s delay time, the entire population of the protein would be unfolded and would come close to reaching the equilibrium distribution among the three D_i substates. The refolding jump gave a kinetic record closely resembling that of folding by the single-jump experiment. If, on the other hand, the delay time were shortened, signals recovered in the refolding jump would be smaller and the relative amplitudes of the three kinetic phases would be different from those of the single-jump experiment. This is because a limited time kept in the unfolded condition would not allow those unfolded proteins to reach the equilibrium distribution among the three substates of D. In oscillograph b of Figure 2, several kinetic traces indicating the refolding to pH 7.0 after incomplete unfolding to pH 3.0, with the delay times of 1.0, 0.8, 0.5, and 0.3 s (in the order from the uppermost to the lowermost trace, respectively), are shown for the first 8 s. Similar experiments done on the alkaline side are shown in oscillograph b of Figure 3. The slower kinetic phase in the refolding jump, with the delay time of 10 s, is shown in oscillographs c of Figure 2 for folding from acid and Figure 3 for folding from alkali. The slow kinetics in refolding jumps with shorter delay times than those specified in oscillographs c are shown in oscillographs d. From these kinetic records, it is clear that the recovery of the fluorescence signals in the refolding jump depended on the time (t_D) that the protein sample was kept at the unfolding condition. The relative amplitudes of the three kinetic phases in the refolding jump as a function of the delay time reflect the rates of unfolding of the three steps, as would be expected for Scheme I. In order to perform the detailed analysis outlined later, we have arranged the data as follows. The kinetic records of the refolding jump in the first 5 s were deconvoluted into two exponential decay constants. The relative amplitude of the dominant phase was normalized to the maximal fluorescence signal (when t_D = 50 s for refolding from acid and 30 s from alkali). The normalized amplitude is plotted against the delay time (filled circles) in Figures 4a and 5a, respectively, for the refolding from pH 3.0 and from pH 12.2 to the final pH 7.0. The relative amplitude of the second reaction is plotted against

Table I: Experimental Data and Kinetic Parameters Obtained by Model Analysis[a]

	acidic side		alkaline side	
	experiment	theory	experiment	theory
	Unfolding from pH 7.0 to pH 3.0 or 12.2			
τ_{u1} (s)	1.07		0.60	
τ_{u2} (s)	0.047		0.10	
τ_{u3} (s)	10.0		5.0	
u_{01} (s^{-1})		0.93		1.67
u_{12} (s^{-1})		6.68		4.12
u_{21} (s^{-1})		14.40		5.88
u_{23} (s^{-1})		0.033		0.13
u_{32} (s^{-1})		0.091		0.14
C_{u0}(eq)		0.00		0.00
C_{u1}(eq)		0.61		0.43
C_{u2}(eq)		0.28		0.30
C_{u3}(eq)		0.11		0.27
	Refolding from pH 3.0 or 12.2 to pH 7.0			
τ_{f1} (s)	0.15		0.091	
τ_{f2} (s)	0.87		0.57	
τ_{f3} (s)	30.0		33.0	
r_{10} (s^{-1})		6.62		11.1
r_{21} (s^{-1})		1.16		1.77
r_{32} (s^{-1})		0.33		0.31
A_0(eq)	0.0		0.0	
A_1(eq)	0.55		0.37	
A_2(eq)	0.34		0.35	
A_3(eq)	0.11		0.28	
B_{00}		0.0		0.0
B_{10}		0.55		0.37
B_{20}		0.34		0.35
B_{30}		0.11		0.28
B_{11}	−0.53	−0.60	−0.41	−0.41
B_{12}	−0.016	−0.018	−0.098	−0.098
B_{13}	0.0	0.065	0.0	0.14
B_{21}	−0.37	−0.40	−0.59	−0.59
B_{22}	0.016	0.018	0.098	0.098
B_{23}	0.0	0.045	0.0	0.14
B_{31}	0.0	0.0	0.0	0.0
B_{32}	0.0	0.0	0.0	0.0
B_{33}	−0.11	−0.11	−0.28	−0.28

[a] τ_{ui} values are relaxation times for unfolding, experimentally determined through the analysis of the refolding jumps (see eq A8). τ_{fi} values are the relaxation times for folding measured directly from the kinetic records. C_{ui}(eq) values, equilibrium concentrations of C_i in unfolding, were determined by eq A12. r_i values, rate constants in refolding, were determined by eq 3. A_i(eq) values, amplitudes of different kinetic phases when t_D is approaching infinity, were experimentally determined (see eq A8). B_{ij} values are coefficients defined in eq A8 and were determined by regression analysis of data in Figures 4 and 5 in refolding jumps according to eq A8. These values were also calculated, theoretically, from eqs A9, A10, and A11. u_{ij} values were calculated from eq A13. Kinetic measurements were done at 25 °C. The uncertainty in these experiments was ±3% for the amplitudes and ±5% for the relaxation times.

the delay time (open circles) in the same figures. The slower kinetics in the refolding jump were fit into a single-exponential curve, and the amplitude as a function of t_D is shown in Figures 4b and 5b for folding from acid and alkali, respectively. The maximal amplitudes of this slow kinetic phase constituted roughly 11% in the folding from acid and 28% in the folding from alkali (Chen et al., 1991). The complete sets of kinetic constants for folding and unfolding, both for the acid side and for the alkaline side, are listed in Table I. Detailed kinetic analysis based on the data obtained in the direct pH jump (Chen et al., 1991) and those presented here (see the following section and Table I) yielded solid curves shown in Figures 4 and 5. The good fit in Figure 4 indicates that Scheme I is a good description of the folding/unfolding of the protein for the acidic side. The fit of kinetic data for the alkaline side (Figure 5) was not as good (see Discussion).

Relaxation times for both the folding and unfolding were also measured at different temperatures to determine the activation energy. A complete set of experimentally determined relaxation times and their activation energies are listed in Table II.

Kinetic Analysis. The analysis presented here was for the folding to a strongly native condition (e.g., 0.125 M NaCl, 25 °C, at pH 7.0) and the unfolding to a strongly denaturing condition (e.g., 0.125 M NaCl, 25 °C, pH 3.0 or 12.2). With this assumption, the unfolding of Scheme I, as in the first pH jump, can be approximated by Scheme II. Likewise, the

Scheme II

$$N_0 \xrightarrow{u_{01}} D_1 \underset{u_{21}}{\overset{u_{12}}{\rightleftharpoons}} D_2 \underset{u_{32}}{\overset{u_{23}}{\rightleftharpoons}} D_3$$

folding of Scheme I, as in the second jump, can be approximated by Scheme III. In these schemes, u_{ij} denotes the rate

Scheme III

$$N_0 \xleftarrow[r_{10}]{} D_1 \xleftarrow[r_{21}]{} D_2 \xleftarrow[r_{32}]{} D_3$$

of transition from species i to species j at a denaturing condition, and r_{ij} denotes the rate of transition from species i to species j at a native condition. The choice of strongly native and denaturing conditions implies that u_{10}, r_{01}, r_{12}, and r_{23} would be negligibly small compared to their corresponding reverse rates. Thus, these rate constants were neglected in the analysis. This means that the N_0 to D_1 transition for the unfolding and all three reactions for the folding are nearly unidirectional. On the other hand, transitions between different D_i states in the unfolding would be reversible because these states have similar stabilities.

As will be shown in the appendix, a set of four differential equations can be set up for Scheme II and similarly for Scheme III. Solutions to these differential equations allow calculation of the concentration of any species at any time. The first unfolding jump always starts with concentrations $C_{u0} = 1$ and $C_{u1} = C_{u2} = C_{u3} = 0$. These concentrations change with t_D, but only the C_{u0} to C_{u1} transition would be associated with fluorescence changes. In other words, $\Delta F(t) \propto C_{u0}(t)$, where

Table II: Activation Energies of pH-Induced Folding/Unfolding of Staphylococcal Nuclease[a]

	Folding to pH 7.0					
	τ_{f1} (ms)	$E_a(\tau_{f1})$ (kcal mol^{-1})	τ_{f2} (ms)	$E_a(\tau_{f2})$ (kcal mol^{-1})	τ_{f3} (s)	$E_a(\tau_{f3})$ (kcal mol^{-1})
from pH 3.0	151	6.0	865	5.6	30	13.4
from pH 12.2	90	6.9	565	6.4	33	13.5
	Unfolding from pH 7.0					
	τ_{u1} (s)	$E_a(\tau_{u1})$ (kcal mol^{-1})	τ_{u2} (ms)	$E_a(\tau_{u2})$ (kcal mol^{-1})	τ_{u3} (s)	$E_a(\tau_{u3})$ (kcal mol^{-1})
to pH 3.0	1.10	27.6	47	8.7	10	13.3
to pH 12.2	0.60	36.8	100	5.8	5.0	12.3

[a] The three relaxation times of refolding (τ_{fi}) were determined by the direct pH jump while those of unfolding (τ_{ui}) were determined by the analysis of the refolding jump by the sequential pH jump method, at 25 °C. Activation energies were determined in the temperature range 15–40 °C. See legends to Figures 4 and 5 and the appendix for details. The uncertainty for the activation energies was ±10%.

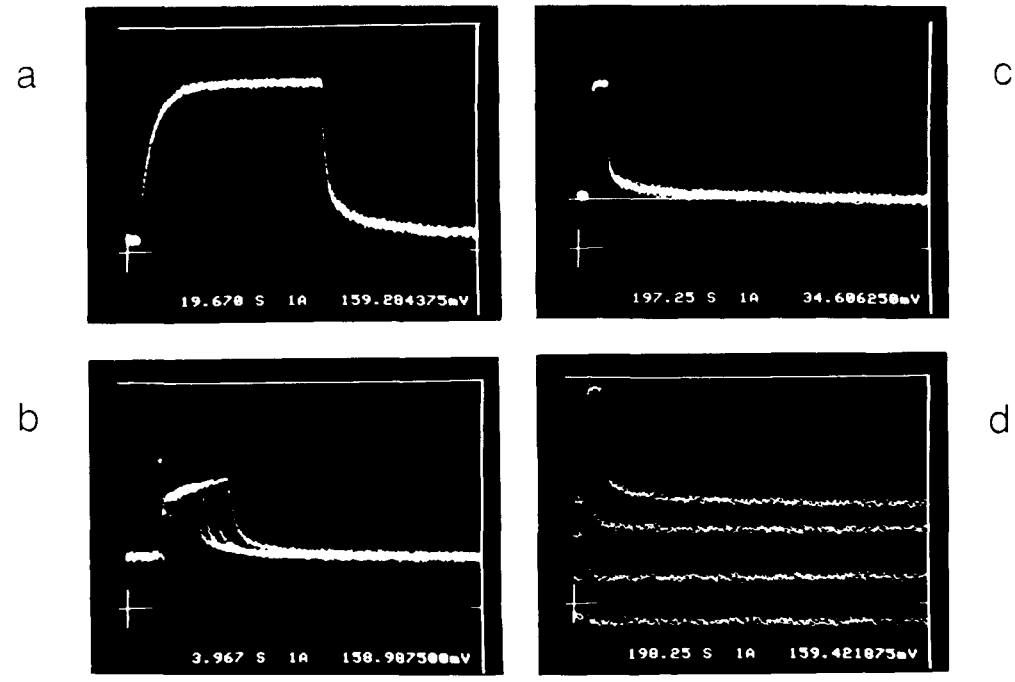

FIGURE 3: Kinetic records of the alkaline-induced folding/unfolding transitions by the sequential pH jumps. (a) A protein solution at pH 7.0 was mixed with a buffer of pH 12.7 to a final pH of 12.2. After 10 s (t_D), the mixture was mixed with a buffer at pH 1.8, which brought the pH of the final solution to 7.0. The upward signal recorded the unfolding and the downward signal recorded the refolding. (b) Kinetic records similar to that in (a) except that t_D were 0.6, 0.5, 0.4, and 0.3 s for the upper to the lower traces, respectively, are shown. The total recording time for the refolding was 4 s. (c) The slow kinetic phase in the refolding jump with a t_D of 10 s is shown. The total recording time was 200 s. (d) More traces are shown for the slow kinetic phase in the refolding jump, with t_D of 10, 3, 1, and 0.5 s, from the upper to the lower traces, respectively. Temperature was 25 °C.

F denotes the fluorescence intensity of Trp-140. During the refolding after the second jump, the concentration of these species, denoted by C_{r0}, C_{r1}, C_{r2}, and C_{r3}, could start at different values depending on t_D, but the final equilibrium concentrations would be $C_{r0} = 1$ and $C_{r1} = C_{r2} = C_{r3} = 0$. Here again, only the transition from C_{r1} to C_{r0} would be associated with fluorescence changes, i.e., $\Delta F(t) \propto C_{r0}$.

To simplify the analysis further, we also took into consideration the experimental observations that

$$(u_{23} + u_{32}) \ll u_{01} \quad \text{or} \quad (u_{12} + u_{21}) \tag{1}$$

Under these conditions, the three relaxation times (τ_{ui}) in the unfolding jump expressed in terms of the rate constants are

$$\tau_{u1}^{-1} = u_{01} \tag{2a}$$

$$\tau_{u2}^{-1} = u_{12} + u_{21} \tag{2b}$$

$$\tau_{u3}^{-1} = u_{32} + u_{12}u_{23}/(u_{12} + u_{21}) \tag{2c}$$

and the three relaxation times in the refolding jump (τ_{fi}) are

$$\tau_{f1}^{-1} = r_{10} \tag{3a}$$

$$\tau_{f2}^{-1} = r_{21} \tag{3b}$$

$$\tau_{f3}^{-1} = r_{32} \tag{3c}$$

Experimental data on the direct pH jump in both folding and unfolding directions (Chen et al., 1991) and the sequential-jump data of Figures 4 and 5 are used for kinetic analysis to obtain a complete set of rate constants and equilibrium concentrations of all four species of protein at pH 3.0 and pH 12.2 (Table I).

In the second column of Table I, data on acidic unfolding are given. The numerical values used to simulate the theoretical curves in Figure 3 are given in the third column. The three relaxation times (τ_{fi}) in refolding were obtained by the single-jump experiment from acid to pH 7.0 (Chen et al., 1991). Their reciprocals give the corresponding rate constants for refolding (r_{ij}) shown in the second column. The first relaxation time in unfolding (τ_{u1}) was obtained by the single unfolding jump to pH 3.0, and the second and third relaxation times (τ_{u2} and τ_{u3}) were determined by the analysis of kinetic records for the second refolding jump shown in Figure 3 by regression analysis according to eq A8 in the appendix. The equilibrium distribution values of the three substates of the denatured state (D_i), which are expressed as the amplitude, A_i(eq), and B_{i0}, i.e., [D_i] at pH 3.0 (see appendix for their physical meanings), inferred from the previous study (Chen et al., 1991), given as 0.55, 0.34, and 0.11 for D_1, D_2, and D_3, respectively, are compared with the theoretical values [C_{ui}(eq)] of 0.61, 0.28, and 0.11, respectively. The agreement is excellent. B_{ij} values in the third column are the coefficients which determine the amplitudes of the three kinetic phases in the refolding jump (A_i). Experimentally, B_{ij} values were obtained by fitting the three kinetic curves of Figure 3 with the nonlinear least-squares method as was done for τ_{ui} (column 2). Theoretical values were obtained as outlined in the appendix. The four rate constants at pH 3.0, u_{12}, u_{21}, u_{23}, and u_{32}, were determined to be 6.68, 14.35, 0.03, and 0.09 s^{-1}, respectively (column 3).

The fourth and the fifth columns compare the experimental observations and the results of the kinetic fit in the alkaline unfolding, as described above for the acidic folding/unfolding. Again, the calculated fractions of D_i at pH 12.2, 0.43, 0.30, and 0.27 for D_1, D_2, and D_3, respectively, compare favorably with the experimentally determined values of 0.37, 0.35, and 0.28. The four experimentally inaccessible rate constants at pH 12.2, u_{12}, u_{21}, u_{23}, and u_{32}, were determined to be 4.12, 5.88, 0.13, and 0.14 s^{-1}, respectively.

Discussion

The thermal stability of staphylococcal nuclease at pH 7 (T_m = 53.3 °C and ΔH_{cal} = 85.3 kcal mol^{-1}) is comparable

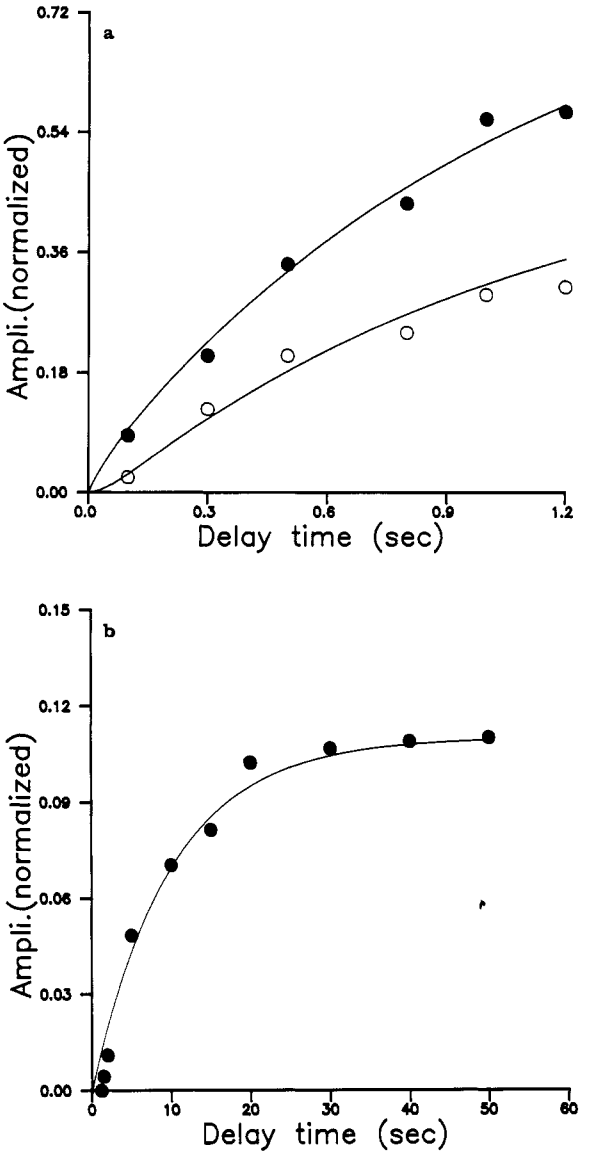

FIGURE 4: Normalized amplitudes of the three kinetic phases in the refolding jump from acid as a function of the delay time, t_D. The kinetic record between 2 ms to 5 s was fit into two exponential decays (τ_{f1} and τ_{f2}) and that of 5 s to 300 s was fit into a single-exponential decay (τ_{f3}). The normalized amplitude of each kinetic phase (total amplitude of a given t_D as unity) was plotted against t_D. In (a), the amplitudes of the τ_{f1} reaction are shown in closed circles and those of the τ_{f2} reaction are shown in the open circles. In (b), the amplitudes of the τ_{f3} reaction are given. The solid curves drawn across the data points were obtained as follows. First, three relaxation times in unfolding, τ_{ui} (column 2 of Table I), were obtained by a least-squares fit of data in both (a) and (b) to eq A8. Second, B_{ij} values (column 3 of Table I) were calculated according to eq A9. The A8 equations were then used to calculate these curves. Another approach used the regression analysis of data in (a) and (b) to simultaneously determine τ_{ui} and B_{ij} (column 2 of Table I). The B_{ij} values obtained by both methods agree.

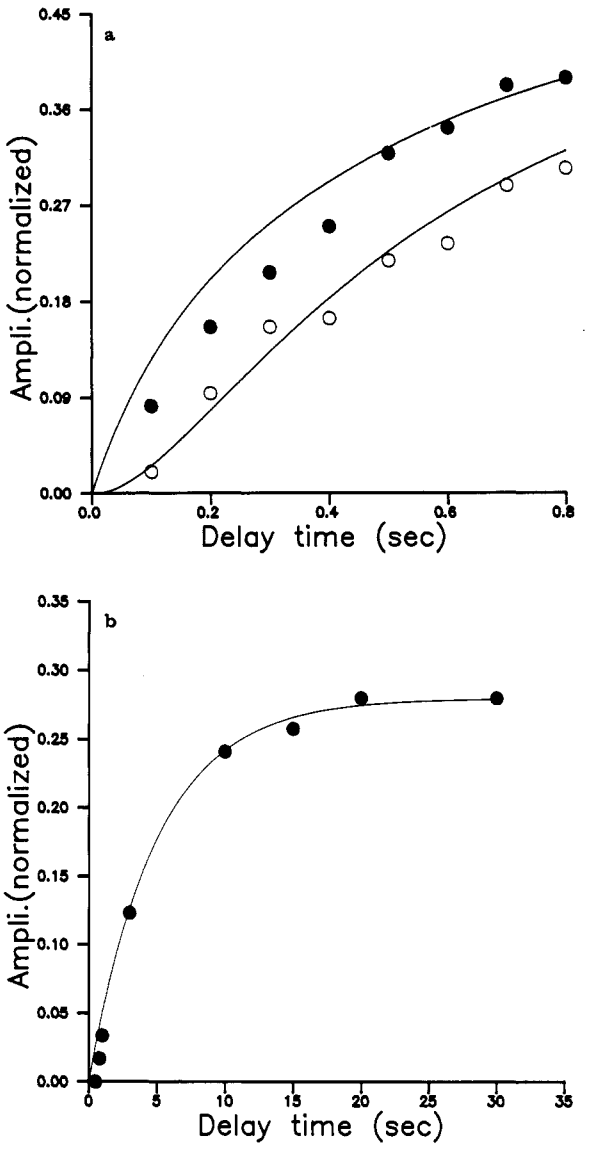

FIGURE 5: Normalized amplitudes of the three kinetic phases in the refolding jump from alkali as a function of the delay time, t_D. The solid curves were calculated by the procedures outlined in Figure 4.

to that of many small proteins (Griko et al., 1988; Privalov, 1979). The protein is also remarkably sensitive to the pH of the solution. At 25 °C, it can be denatured by acid (midpoint pH 3.9) or alkali (midpoint pH 10.5), alone. This indicates that electrostatic interactions play an important role in the protein's stability (Matthew & Gurd, 1986; Gilson & Honig, 1988). Both the acid- and the alkaline-denatured states exhibit residual structures which give CD spectra resembling that of a protein with 40–50% β-sheets (Chen et al., 1991). Notwithstanding, there is no enthalpy of stabilization associated with these residual structures. In other words, these "structures" cannot be removed by heating, although they can be removed by 2 M guanidine hydrochloride (Chen et al., 1991). Many studies have found that the fluorescence intensity of Trp-140 reflects protein stability [see, e.g., Shortle (1989)]. The fluorescence intensity of the native protein is reduced by 85% when it is denatured by heat, acid, or alkali. There is a correlation between the Trp-140 fluorescence and the ΔH_{cal} of unfolding (Chen et al., 1991). The Trp-140 fluorescence values of these three substates are the same, and so are their enthalpies. The free energy difference between D_1 and D_2 is a mere −0.45 kcal mol^{-1} [$\Delta G = -RT \ln(C_{u1}/C_{u2})$] and that between D_2 and D_3 is −0.55 kcal mol^{-1} at pH 3.0. At pH 12.2, the free energy difference among these substates is even smaller (less than 0.2 kcal mol^{-1} between any two species). Thus, these substates are isoenergetic and are populated in the unfolding conditions. The conversion between D_1 and D_2 takes approximately 100 ms, and between D_2 and D_3 it takes approximately 10 s. These results indicate that, at an early stage of the SNase folding, the pathway is determined by kinetic barriers (6–14 kcal mol^{-1}) rather than by the differences in the thermodynamic stabilities of the intermediate states. Note that Hagerman et al. (1979) have reported a stopped-flow sequential jump study of the pH-induced folding/unfolding

transitions of ribonuclease A. Their results are remarkably similar to the data presented here for the SNase. They have used the sequential-jump method to investigate the properties of a transient kinetic intermediate, I_3, which occurs in the 10-ms time range, has absorption similar to unfolded states, and cannot be detected by the direct unfolding jump.

Although any mechanisms of a chemical reaction cannot be rigorously proved by kinetic analysis alone, two observations lend strong support to the proposed mechanisms. First, the calculated amplitudes of the three different kinetic phases in refolding as a function of the delay time t_D (solid curves in Figures 4 and 5) agreed well with the experimental data. The sigmoidal shape of τ_{f2} (open circles) was also faithfully produced (Figures 4a and 5a). Second, B_{ij} values (Table I) obtained by the amplitude analysis of refolding kinetics agreed surprisingly well with the calculated values. Since the calculation of many undetermined kinetic parameters from experimentally accessible parameters is quite complex and necessarily depends on models, the agreement cannot be construed as coincidental. Note, however, that the theoretical fit was less satisfactory on the alkaline side (Figure 5a) compared to that on the acidic side (Figure 4a). This reflects the fact that, in the alkaline unfolding, 60% of the equilibrium signals was completed in the 2-ms mixing time of the stopped-flow instrument (Chen et al., 1991). In all other jumps, more than 90% of equilibrium signals was resolved in the 2 ms to 300 s time range covered in this study (Chen et al., 1991). This suggests that, in the alkaline side, one additional kinetic intermediate has to be included in Scheme I.

Recent NMR studies by Alexandrescu et al. (1989) suggest that the native state of SNase is composed of three substrates in slow equilibrium. The existence of such substates in the native state would result in complex kinetics for the unfolding (Chen et al., 1991). This was not detected in our unfolding to pH 3.0 and pH 12.2. A plausible explanation is that these substates of the native state are unstable under strongly denaturing conditions and their rates of interconversions are very rapid at pH 3.0 and pH 12.2. Our recent result would support such an interpretation (Chen et al., manuscript in preparation). Note also that the protein concentrations and solvent conditions used in the two studies were different.

The nature of the three substates of the denatured form is of considerable interest. The D_3 to D_2 transition has an activation energy of 14 kcal mol^{-1} and a relaxation time of 30 s. This relaxation time is independent of pH in the range 6–9. These results suggest that it is the cis/trans isomerization of one or more of the proline residues (Kim & Baldwin, 1982, 1990). The D_2 to D_1 transition depends on solvent viscosity and may belong to a chain-condensation reaction (Chen et al., manuscript in preparation). We propose that D_2 is an extended form and D_1 is a compact form of the denatured state (Stigter et al., 1991; Kanehisa & Tsong, 1978). The existence of different forms of unfolded proteins as well as intermediates of different physical characteristics in folding has been detected in many recent studies (Goto & Fink, 1989; Ptitsyn, 1987; Baum et al., 1989; Kuwajima, 1989; Kim & Baldwin, 1990). Our data are consistent with some of their observations.

ACKNOWLEDGMENTS

We thank C. J. Gross for help with the manuscript.

APPENDIX: ANALYSIS OF THE KINETIC SCHEME $D_3 \rightleftharpoons D_2 \rightleftharpoons D_1 \rightleftharpoons N_0$

Kinetic Model. This analysis is to use the data obtained by the double-jump method to derive rate constants for the sequential four-state model, following the classical kinetic treatments of Szabo (1969). Specific consideration was given for the facts that in the present analysis the fluorescence changes occurred only in the D_1 to N_0 transition and that kinetics of folding/unfolding were measured at different pHs. The first jump, i.e., the unfolding jump, leads to a strongly denaturing condition (pH 3.0 or pH 12.2; 25 °C). The model is represented by Scheme II. The second jump, i.e., the refolding jump, leads to a strongly native condition (pH 7.0; 25 °C). The model is represented by Scheme III. The rate constants from the i to j species are not the same for the folding (r_{ij}) and the unfolding (u_{ij}) because the pHs of the final conditions are different. An experiment was always started with $C_{u0} = 1$ and $C_{u1} = C_{u2} = C_{u3} = 0$, and the concentration of each species during the unfolding, $C_{ui}(t)$, can be calculated by solving a set of four differential equations for Scheme II with the approximations specified in eqs 1 and 2.

$$\left.\begin{aligned} C_{u0}(t) &= \exp(-t/\tau_{u1}) \\ C_{u1}(t) &= (U_{12}U_{23}/\beta) - [(\alpha - U_{12})/(\alpha - \gamma)] \exp(-t/\tau_{u1}) \\ &\quad + [\alpha/(\alpha\gamma - \gamma^2)] \exp(-t/\tau_{u2}) + (U_{12}/\beta\gamma) \exp(-t/\tau_{u3}) \\ C_{u2}(t) &= U_{23}/\beta + [1/(\alpha - \gamma)] \exp(-t/\tau_{u1}) \\ &\quad - [\alpha/(\alpha\gamma - \gamma^2)] \exp(-t/\tau_{u2}) + (1/\beta\gamma) \exp(-t/\tau_{u3}) \\ C_{u3}(t) &= (1/\beta)[1 - \exp(-t/\tau_{u3})] \end{aligned}\right\} \quad \text{(A1)}$$

In these equations $\alpha = u_{01}/u_{12}$ and $\beta = 1 + U_{23} + U_{12}U_{23}$ and $\gamma = 1 + U_{12}$, and the equilibrium constants $U_{12} = u_{21}/u_{12}$ and $U_{23} = u_{32}/u_{23}$. When t approaches infinity, eq A1 gives equilibrium concentration $[C_{ui}(\text{eq})]$ of each species in a strongly denaturing condition.

$$\begin{aligned} C_{u0}(\text{eq}) &= 0 \qquad C_{u1}(\text{eq}) = U_{12}U_{23}/\beta \\ C_{u2}(\text{eq}) &= U_{23}/\beta \qquad C_{u3}(\text{eq}) = 1/\beta \end{aligned} \quad \text{(A2)}$$

Similarly, four differential equations can be set up for Scheme III. The initial concentration for each species, or the concentration at $t = t_D$, for the refolding will be

$$C_{ri}(t_D) = C_{ui}(t_D) \qquad i = 0, 1, 2, \text{ or } 3 \quad \text{(A3)}$$

The three relaxation times of the refolding jump are shown in eq 3. It can be shown that

$$\left.\begin{aligned} C_{r0}(t) &= 1 - [C_{u1}(t_D) - r_{21}\delta/(r_{10} - r_{21})] \exp[-(t - t_D)/\tau_{f1}] \\ &\quad - [r_{10}\epsilon/(r_{10} - r_{21})] \exp[-(t - t_D)/\tau_{f2}] \\ &\quad - \{r_{10}r_{21}C_{u3}(t_D)/[(r_{10} - r_{32})(r_{21} - r_{32})]\} \exp[-(t - t_D)/\tau_{f3}] \\ C_{r1}(t) &= [C_{u1}(t_D) - r_{21}\delta/(r_{10} - r_{21})] \exp[-(t - t_D)/\tau_{f1}] \\ &\quad + [r_{21}\epsilon/(r_{10} - r_{21})] \exp[-(t - t_D)/\tau_{f2}] \\ &\quad + \{r_{21}r_{32}C_{u3}(t_D)/[(r_{10} - r_{32})(r_{21} - r_{32})]\} \exp[-(t - t_D)/\tau_{f3}] \\ C_{r2}(t) &= \epsilon \exp[-(t - t_D)/\tau_{f2}] + [r_{32}C_{u3}(t_D)/(r_{21} - r_{32})] \exp[-(t - t_D)/\tau_{f3}] \\ C_{r3}(t) &= C_{u3}(t_D) \exp[-(t - t_D)/\tau_{f3}] \end{aligned}\right\} \quad \text{(A4)}$$

In these equations, $\delta = C_{u2}(t_D) - r_{32}C_{u3}(t_D)/(r_{10} - r_{32})$ and $\epsilon = C_{u2}(t_D) - r_{32}C_{u3}(t_D)/(r_{21} - r_{32})$.

Experimental and Theoretical Determination of Kinetic Parameters. The normalized fluorescence intensity, $\Delta F(t)$, is dependent only on $C_0(t)$.

$$\Delta F(t) \approx C_0(t) \quad \text{(A5)}$$

For the unfolding, the fluorescence change has only one decay constant, τ_{u1}.

$$\Delta F_u(t) = \exp(-t/\tau_{u1}) \quad \text{(A6)}$$

A direct unfolding jump to pH 3.0 or 12.2, which is monophasic, allowed τ_{u1} to be determined. The second jump, or the refolding jump, however, was triphasic, and the complete time course of the fluorescence change would be

$$\Delta F_r(t) = 1 - A_1(t_D)\exp[-(t - t_D)/\tau_{f1}] - A_2(t_D)\exp[-(t - t_D)/\tau_{f2}] - A_3(t_D)\exp[-(t - t_D)/\tau_{f3}] \quad (A7)$$

Both amplitudes (A_i) and relaxation times (τ_{fi}) can be determined experimentally. The three relaxation times depend only on the final pH (7.0), and their values are given in Table I. On the other hand, the amplitude of each kinetic phase in refolding depended on t_D.

$$\left.\begin{aligned} A_1(t_D) &= B_{10} + B_{11}\exp(-t_D/\tau_{u1}) + B_{12}\exp(-t_D/\tau_{u2}) + B_{13}\exp(-t_D/\tau_{u3}) \\ A_2(t_D) &= B_{20} + B_{21}\exp(-t_D/\tau_{u1}) + B_{22}\exp(-t_D/\tau_{u2}) + B_{23}\exp(-t_D/\tau_{u3}) \\ A_3(t_D) &= B_{30} + B_{31}\exp(-t_D/\tau_{u1}) + B_{32}\exp(-t_D/\tau_{u2}) + B_{33}\exp(-t_D/\tau_{u3}) \end{aligned}\right\} \quad (A8)$$

It can be shown that the amplitudes of different kinetic phases in refolding jumps according to Schemes II and III are

$$\left.\begin{aligned} B_{10} &= (1/\beta)\{U_{12}U_{23} - r_{21}(r_{10}U_{23} - r_{32} - r_{32}U_{23})/[(r_{10} - r_{21})(r_{10} - r_{32})]\} \\ B_{11} &= -[1/(\alpha - \gamma)][\alpha - U_{12} + r_{21}/(r_{10} - r_{21})] \\ B_{12} &= r_{10}\alpha/[(\alpha\gamma - \gamma^2)(r_{10} - r_{21})] \\ B_{13} &= (1/\beta\gamma)\{U_{12} - [r_{21}(r_{10} - r_{32}U_{12})]/[(r_{10} - r_{21})(r_{10} - r_{32})]\} \\ B_{20} &= r_{10}(r_{21}U_{23} - r_{32} - r_{32}U_{23})/[\beta(r_{10} - r_{21})(r_{21} - r_{32})] \\ B_{21} &= r_{10}/[(\alpha - \gamma)(r_{10} - r_{21})] \\ B_{22} &= -r_{10}\alpha/[(\alpha\gamma - \gamma^2)(r_{10} - r_{21})] \\ B_{23} &= r_{10}(r_{21} + r_{32}U_{12})/[\beta\gamma(r_{10} - r_{21})(r_{21} - r_{32})] \\ B_{30} &= r_{10}r_{21}/[\beta(r_{10} - r_{32})(r_{21} - r_{32})] \\ B_{31} &= 0 \\ B_{32} &= 0 \\ B_{33} &= -r_{10}r_{21}/[\beta(r_{10} - r_{32})(r_{21} - r_{32})] \end{aligned}\right\} \quad (A9)$$

When t_D approaches infinity, the unfolded state will be in equilibrium and, from eq A8, one obtains

$$A_1(\text{eq}) = B_{10} \qquad A_2(\text{eq}) = B_{20} \qquad A_3(\text{eq}) = B_{30} \quad (A10)$$

Thus, these three B values were assigned with the experimentally determined values for A_i(eq) (see Table I, columns 3 and 5). The sum of these three values should be equal to unity. Expressions for these B values contain U_{12} and U_{23} and rate constants for refolding but no rate constants for unfolding. The three rate constants for refolding are experimentally measured (see eq 3). Thus, U_{12} and U_{23} can be determined by solving any two relationships of eq A10.

$$\left.\begin{aligned} U_{12} &= \frac{r_{21}[A_1(\text{eq})r_{10} + A_2(\text{eq})r_{21} + A_3(\text{eq})r_{32}]}{A_2(\text{eq})r_{21}(r_{10} - r_{21}) + A_3(\text{eq})r_{32}(r_{10} - r_{32})} \\ U_{23} &= \frac{A_2(\text{eq})r_{21}(r_{10} - r_{21}) + A_3(\text{eq})r_{32}(r_{10} - r_{32})}{A_3(\text{eq})(r_{10} - r_{32})(r_{21} - r_{32})} \end{aligned}\right\} \quad (A11)$$

All C_{ui}(eq) values can then be expressed by experimentally accessible rate constants and amplitudes using eq A1 as t approaches infinity.

$$\left.\begin{aligned} C_{u0}(\text{eq}) &= 0 \\ C_{u1}(\text{eq}) &= A_1(\text{eq}) + A_2(\text{eq})(r_{21}/r_{10}) + A_3(\text{eq})(r_{32}/r_{10}) \\ C_{u2}(\text{eq}) &= A_2(\text{eq})(1 - r_{21}/r_{10}) + A_3(\text{eq})(r_{32}/r_{21})(1 - r_{32}/r_{10}) \\ C_{u3}(\text{eq}) &= A_3(\text{eq})(1 - r_{32}/r_{10})(1 - r_{32}/r_{21}) \end{aligned}\right\} \quad (A12)$$

Calculated values for C_{ui} are listed in columns 3 and 5 of Table I.

Likewise, the kinetic constants u_{ij} can also be expressed in the experimentally accessible parameters τ_{ui}, A_i(eq), and r_{ij}, by solving eqs 2 and A11.

$$\left.\begin{aligned} U_{01} &= 1/\tau_{u1} \\ U_{12} &= \frac{1}{\tau_{u2}}\,\frac{A_2(\text{eq})r_{21}(r_{10} - r_{21}) + A_3(\text{eq})r_{32}(r_{10} - r_{32})}{[A_1(\text{eq})r_{10}r_{21} + A_2(\text{eq})r_{10}r_{21} + A_3(\text{eq})r_{32}(r_{10} + r_{21} - r_{32})]} \\ U_{21} &= \frac{1}{\tau_{u2}}\,\frac{r_{21}[A_1(\text{eq})r_{10} + A_2(\text{eq})r_{21} + A_3(\text{eq})r_{32}]}{[A_1(\text{eq})r_{10}r_{21} + A_2(\text{eq})r_{10}r_{21} + A_3(\text{eq})r_{32}(r_{10} + r_{21} - r_{32})]} \\ U_{23} &= (1/\tau_{u3})[A_3(\text{eq})(r_{10} - r_{32})(r_{21} - r_{32})/(r_{10}r_{21})] \times \frac{A_1(\text{eq})r_{10}r_{21} + A_2(\text{eq})r_{10}r_{21} + A_3(\text{eq})r_{32}(r_{10} + r_{21} - r_{32})}{A_2(\text{eq})r_{21}(r_{10} - r_{21}) + A_3(\text{eq})r_{32}(r_{10} - r_{32})} \\ U_{32} &= (1/\tau_{u3})[A_1(\text{eq})r_{10}r_{21} + A_2(\text{eq})r_{10}r_{21} + A_3(\text{eq})r_{32}(r_{10} + r_{21} - r_{32})]/(r_{10}r_{21}) \end{aligned}\right\} \quad (A13)$$

Thus, all rate constants and, hence, the equilibrium constants in Schemes II and III can be unambiguously resolved from the experimental data. These values are listed in columns 3 and 5 of Table I. The solid curves in Figures 4 and 5 were calculated using these kinetic parameters. The agreement is excellent considering the complexity of the analysis.

References

Alexandrescu, A. T., Ulrich, E. L., & Markley, J. L. (1989) *Biochemistry 28*, 204–211.

Baum, J., Dobson, C. M., Evans, P. A., & Hanley, C. (1989) *Biochemistry 28*, 7–13.

Brandts, J. F., Halvorson, H. R., & Brennan, M. (1975) *Biochemistry 14*, 4953–4963.

Chen, H. M., You, J. L., Markin, V. S., & Tsong, T. Y. (1991) *J. Mol. Biol. 220*, 771–778.

Davis, A., Parr, G. R., & Taniuchi, H. (1979) *Biochim. Biophys. Acta 578*, 505–510.

Epstein, H. F., Schechter, A. H., Chen, R. F., & Anfinsen, C. B. (1971) *J. Mol. Biol. 60*, 499–508.

Fuchs, S., Cuatrecasas, P., & Anfinsen, C. B. (1967) *J. Biol. Chem. 242*, 4768–4770.

Gilson, M. K., & Honig, B. H. (1988) *Proteins: Struct., Funct., Genet. 4*, 7–18.

Goto, Y., & Fink, A. L. (1989) *Biochemistry 28*, 945–952.

Griko, Y. V., Privalov, P. L., Sturtevant, J. M., & Venyaminov, S. Y. (1988) *Proc. Natl. Acad. Sci. U.S.A. 85*, 3343–3347.

Hagerman, P. J., & Baldwin, R. L. (1976) *Biochemistry 15*, 1462–1473.

Hagerman, P. J., Schmid, F. X., & Baldwin, R. L. (1979) *Biochemistry 18*, 293–297.

Kanehisa, M. I., & Tsong, T. Y. (1978) *J. Mol. Biol. 124*, 177–194.

Kim, P. S., & Baldwin, R. L. (1982) *Annu. Rev. Biochem. 51*, 459–489.

Kim, P. S., & Baldwin, R. L. (1990) *Annu. Rev. Biochem. 59*, 631–660.

Kuwajima, K. (1989) *Proteins: Struct., Funct., Genet. 6*, 87–103.

Marquardt, D. W. (1963) *J. Soc. Ind. Appl. Math. 11*, 431–441.

Matthew, J. B., & Gurd, F. R. N. (1986) *Methods Enzymol. 130*, 413–436.

Nakano, T., & Fink, A. L. (1990) *J. Biol. Chem. 265*, 12356–12362.

Privalov, P. L. (1979) *Adv. Protein Chem. 33*, 167–241.

Ptitsyn, O. B. (1987) *J. Protein Chem. 6*, 273–293.
Schechter, A. N., Chen, R. F., & Anfinsen, C. B. (1970) *Science 167*, 886–887.
Shortle, D. J. (1989) *J. Biol. Chem. 264*, 5315–5318.
Shortle, D., & Meeker, A. K. (1989) *Biochemistry 28*, 936–944.
Stigter, D., Alonso, D. O. V., & Dill, K. (1991) *Proc. Natl. Acad. Sci. U.S.A. 88*, 4176–4180.
Sugawara, T., Kuwajima, K., & Sugai, S. (1991) *Biochemistry 30*, 2698–2706.
Szabo, Z. G. (1969) in *Comprehensive Chemical Kinetics* (Bamford, C. H., & Tipper, C. F. H., Eds.) Vol. 2, Chapter 1, Elsevier, Amsterdam.
Tanford, C. (1968) *Adv. Protein Chem. 23*, 121–282.

Engineering Surface Charge. 1. A Method for Detecting Subunit Exchange in *Escherichia coli* Glutathione Reductase†

Mahendra P. Deonarain, Nigel S. Scrutton, and Richard N. Perham*
Cambridge Centre for Molecular Recognition, Department of Biochemistry, University of Cambridge, Tennis Court Road, Cambridge CB2 1QW, U.K.

Received June 14, 1991; Revised Manuscript Received October 30, 1991

ABSTRACT: The gene *gor* encoding *Escherichia coli* glutathione reductase was mutated to create a positively charged N-terminal extension consisting of five arginine residues followed by a factor Xa cleavage site to the enzyme polypeptide chain. The modified protein assembled in vivo to yield a dimeric enzyme with kinetic parameters indistinguishable from those of wild-type glutathione reductase. The N-terminal extension could not be released by treatment with factor Xa but could be removed by exposure to trypsin, again without effect on the enzyme activity. The modified enzyme was readily separated from the wild-type enzyme by means of ion-exchange chromatography or nondenaturing polyacrylamide gel electrophoresis. Incubation of the modified and wild-type enzymes, separately or as a mixture, with NADH led to their partial inactivation, and activity was restored by exposure to 1 mM reduced glutathione. No hybrid dimer was formed in the mixture of modified and wild-type enzymes, as judged by polyacrylamide gel electrophoresis, strongly suggesting that the inactivation induced by NADH was not due to dissociation of the parental dimers. The addition of otherwise benign positively or negatively charged extensions to the N- or C-terminal regions of the constituent polypeptide chains of oligomeric enzymes offers a simple route to detecting hybrid formation and the causative subunit dissociation and exchange.

The flavoprotein glutathione reductase (EC 1.6.4.2) catalyzes the NADPH-dependent reduction of oxidized glutathione according to the equation:

$$NADPH + GSSG + H^+ \rightleftharpoons 2GSH + NADP^+$$

Reduced glutathione, GSH, plays an important role in almost all cells. For example, it is required to protect against oxidative damage and for the maintenance of reduced thiol groups, and it is crucially involved in the synthesis of deoxyribonucleotides [for reviews, see Holmgren (1985) and Schirmer et al. (1989)].

Glutathione reductase is a dimer of identical subunits, each of which possesses a small intrachain disulfide bridge that, together with enzyme-bound FAD, forms the redox center of the enzyme. It is a member of the family of flavoprotein disulfide oxidoreductases which share the same general mechanistic and structural features. Other members include dihydrolipoamide dehydrogenase (EC 1.8.1.4), an essential component of the 2-oxo acid dehydrogenase multienzyme complexes (Patel & Roche, 1990; Perham, 1991), mercuric reductase, which forms part of a bacterial system for the detoxification of mercuric ions (Fox & Walsh, 1983; Brown et al., 1983; Walsh et al., 1988), and trypanothione reductase, an analogue of glutathione reductase found in trypanosomatids (Shames et al., 1986, 1988; Krauth-Siegel et al., 1987). These enzymes exhibit a high degree of sequence similarity, especially around the redox-active disulfide bridges, suggesting that the proteins have acquired different substrate specificities by divergent evolution from a common ancestor (Perham et al., 1978; Williams et al., 1982; Packman & Perham, 1982; Krauth-Siegel et al., 1982; Fox & Walsh, 1983; Brown et al., 1983; Shames et al., 1988).

The crystallographic structure of human glutathione reductase in the absence and presence of substrates and substrate analogues is known at high resolution (Thieme et al., 1981; Karplus & Schulz, 1987; Pai et al., 1988; Karplus et al., 1989). The NADPH- and GSSG-binding sites are physically distinct and separated (approximately 1.8 nm apart) by the isoalloxazine ring of the enzyme-bound FAD (Thieme et al., 1981; Karplus & Schulz, 1987). Moreover, the GSSG-binding site is composed of amino acid side chains originating from both enzyme subunits (Pai & Schulz, 1983; Karplus et al., 1989), making it inconceivable that monomers of glutathione reductase are active. The structural detail from X-ray crystallography, in conjunction with protein chemical and kinetic analysis, has enabled a detailed reaction mechanism for the enzyme to be proposed (Williams, 1976; Pai & Schulz, 1983; Wong et al., 1988).

The availability of a cloned (Greer & Perham, 1986) and overexpressed (Scrutton et al., 1987; Deonarain et al., 1989)

† This work was supported by the Science and Engineering Research Council and the Cambridge Centre for Molecular Recognition, the Royal Commission for the Exhibition of 1851, and St. John's College, Cambridge. M.P.D. was supported by a research studentship from the SERC and by a benefactors' research scholarship from St. John's College. N.S.S. is a Research Fellow of the Royal Commission for the Exhibition of 1851 and a Research Fellow of St. John's College, Cambridge.
* To whom correspondence should be addressed.

0006-2960/92/0431-1491$03.00/0